Precision of Binary Matching Systems

Roger W. Ehrich
Visvanathan Ramesh

TR 87-17

PRECISION OF BINARY MATCHING SYSTEMS

by

Roger W. Ehrich
Visvanathan Ramesh

CS Technical Report TR 87-17

Departments of Computer Science and Electrical Engineering
Virginia Polytechnic Institute and State University
Blacksburg, Virginia 24061

June 21, 1987

10th IASTED Symposium
on Robotics and Automation
Lugano, CH, June 1987

Precision of Binary Matching Systems

Roger W. Ehrich
Visvanathan Ramesh

Departments of Computer Science and Electrical Engineering
Virginia Polytechnic Institute and State University
Blacksburg, Virginia 24061, USA

ABSTRACT

Inexpensive memory and fast processors have made it feasible to build binary matching inspection systems capable of very high measurement precision that operate at near-camera speeds. While the limitations of binary inspection are well known, its performance and cost advantage can be very large in situations in which it can be applied. When binary matching inspection systems are designed and when they are purchased and installed by end-users it becomes absolutely essential to understand the numerous sources that contribute to measurement error. That makes it possible to make precise statements about the accuracy of components whose tolerances they are used to certify.

This paper considers quantitative precision issues for the inspection of strictly 2-dimensional objects using line scan cameras that integrate while the workpiece is in motion.

1 INTRODUCTION

Binary matching systems are commonly used for industrial inspection because binary algorithms are among the most robust available for vision (Reinhold and VanderBrug, 1980). The matching procedures themselves are straightforward, and with clever hardware and algorithm design, matching can be done at near-camera rates by standard microprocessors. For example, in one system being designed by ICRA (Alterswil, CH), a Compaq Deskpro 386 computer is targeted to match 6,912 × 12,000 pixel images in roughly 30 seconds, which includes a scan time of roughly 10 seconds. The other aspect of binary matching that makes it so attractive is price. Since high performance can be achieved at modest price it becomes feasible to consider automatic inspection in manufacturing stations where the payoff is marginal.

One of the major problems faced by industries seeking to employ automatic inspection devices is that the field of automatic inspection is so specialized. Industries have difficulties understanding the performance and behavior of commercially available inspection devices unless there is a resident staff trained in the technology. Even then, the process of understanding a problem and its possible solutions is frequently a black art. Binary inspection devices have the greatest chance of being made into a standard off-the-shelf product because of their conceptual simplicity. However, this is deceptive. There are a large number of factors that can make binary inspection extremely difficult even when pattern and background can be successfully separated by a simple threshold. It is absolutely essential to obtain an understanding of these factors in order to be able to make guarantees about the quality of workpieces that survive inspection, and it is the purpose of this paper to discuss the sources of error in the matching process and to investigate geometric errors in detail.

The support of this work under Grant INF-86-006 from the Virginia Center for Innovative Technology is gratefully acknowledged.

The model for binary matching systems discussed in this paper is illustrated in Figure 1. A workpiece in its production environment is moved synchronously with a line scanning camera. When the workstation is initialized, a reference workpiece is first scanned by the system, and the resulting image is binarized and stored. Next a design system is used to generate a *don't care* or DC image, which is a binary mask that specifies which pixels are to be ignored during matches without causing a rejection of the workpiece. Subsequent workpieces are scanned and compared with the reference, and any mismatches outside the DC mask initiate rejection. The DC regions are also used for a second purpose that is crucial to the inspection system. DC pixels are distributed on both sides of each object edge to reduce the sensitivity of the system to noise and to control the decision parameters of the system.

This type of system relies on a fixed threshold, rather than on a scene-dependent threshold. This makes it possible to reduce the data rate from the camera, which may be 5 to 10 Mpixels/second if sufficient scene illumination can be provided.

It is unrealistic, especially in high resolution systems, to expect that workpieces can be mechanically positioned to sufficient accuracy. Consequently, after a workpiece is scanned, a reference mark on the workpiece is located in the image, as shown in Figure 1, and compared with an identical one on the reference. This is used to align the reference image with the workpiece before the matching is done.

2 ERROR SOURCES

There are a large number of error sources for binary inspection systems of the type described in the introduction. Although this paper deals primarily with 2-dimensional geometric problems, other errors arise from the fact that most scenes are not strictly two-dimensional and from thresholding problems, including drift, illumination, and threshold instabilities in the imaging system. In this section the nature of these problems is explored and related to accuracy of measurement.

2.1 STATIC or LONG TERM PROBLEMS

Many inspection difficulties are caused by problems with illumination, and frequently binary inspection is selected even though operating conditions make it marginally applicable. In order to avoid long term deterioration of performance, it is important to understand the factors that contribute to the difficulties of binary

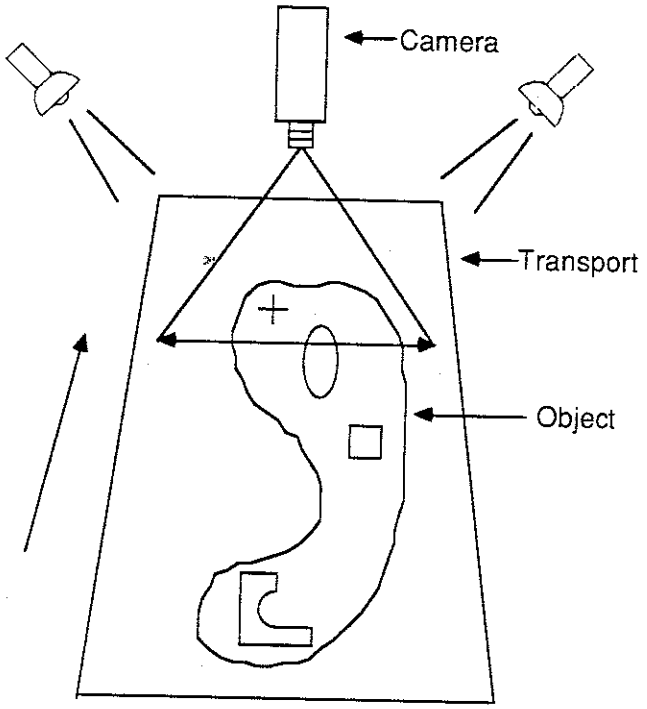

Figure 1 - Inspection Station

vision. Binary inspection systems usually function with one or multiple intensity thresholds that segment the test image into regions. Thresholding may be done at the camera to minimize data transmission rates, or it may be carried out in the vision processor to provide greater flexibility in the vision algorithms. However, the reliable and repeatable segmentation of a scene is extremely sensitive to illumination conditions, scene reflectivity, and electronic stability.

Let us assume that a vision system such as that shown in Figure 1 is illuminated by a source of intensity $I_0(\lambda)$, where λ is the wavelength. Then at the detector, the response will be proportional to

$$I(\lambda) = I_0(\lambda)R(\lambda)S(\lambda)$$

where $R(\lambda)$ is the scene reflectivity and $S(\lambda)$ is the camera sensitivity. The human visual world is one that is primarily illuminated by diffuse light and dominated by the spectral sensitivity characteristics of the human eye. In machine vision, the illumination source is rarely diffuse, and because of the sensor characteristics, the detector response may not coincide with what is seen by the human observer. Finally, the eye is incredibly tolerant of poor image conditions, with the result that there is remarkably poor perception of local behavior of $I_0(\lambda)$ and $R(\lambda)$.

The most important aspect of $I(\lambda)$ is the contrast of a foreground object in comparison with other objects and with background. Contrast may be defined as

$$C = \frac{I_{max} - I_{min}}{I_{max} + I_{min}}$$

where I_{max} is the maximum intensity of a region and I_{min} is the maximum intensity of all the other regions darker than the one of interest. In Figure 2 it can be seen that in order to minimize the sensitivity of position to changes in threshold, the threshold should be set at the maximum slope point of the edge profile. One way to do this is to maximize C by maximizing $\Delta I = I_{max} - I_{min}$. Ultimately, an

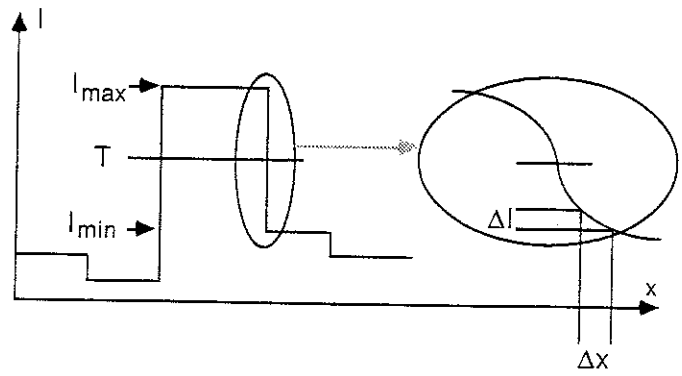

Figure 2 - Region Contrast

unstable threshold is the root of many of the difficulties in binary inspection; it may cause edge position shifts or, in serious cases, complete segmentation failure.

2.1.1 Stability

Over long periods of time it is common for light sources to change intensity as well as spectral composition. Any change in illumination is equivalent to a change in threshold, which causes an error in dimensional measurement. The threshold itself is subject to drift, which has the same effect. Even if power level is held constant, a spectral shift may cause changes to $I(\lambda)$ at wavelengths that are crucial to inspection.

2.1.2 Workpiece Changes

As inspection continues over long production runs, manufacturing materials may change in ways that seem insignificant to the production engineer while being visibly different to the inspection system. This may cause major changes in the behavior of the inspection system that are not noticed by the quality control staff.

2.1.3 Lighting Anomalies

It is notoriously difficult to achieve uniform illumination over wide inspection areas. Even fiberoptic line converters have output that is spatially variant by several percent, and photo arrays exhibit similar behavior. Therefore, even though materials may be absolutely uniform across the field of view, the threshold in different parts of the field may be set at different points on the edge profile, preventing the setting of a uniformly optimal threshold. In severe cases, this may even prevent adequate region segmentation.

Another cause of lighting difficulty is specularity. If point light sources are used to illuminate specular surfaces, the amount of light reflected into the camera lens will vary across a scan line. This may have the effect of changing the contrast across a scan line and consequently the relative position of the threshold in the edge intensity profile. As before this prevents optimal threshold setting for all the image regions, with the result that the dimensional measurements will be susceptible to threshhold variations.

2.1.4 Physical Disturbances

During inspection, physical disturbances to the inspection apparatus, even though minor, will alter the system performance. For example, vibration, shock, or temperature changes may alter the physical alignment of system conponents. Smoke, accumulated dirt, or reflections from objects in the vicinity can cause performance changes.

2.2 DYNAMIC PROBLEMS

In this section the effect of short term random threshold variations is examined in combination with the effect of the continuous state of motion of workpieces normal to the camera scan direction. The development here demonstrates the importance of the difficulties described in Section 2.1. Unlike long term drift problems, these cannot be solved by frequent rescannning of the reference workpiece. Let us assume that the point spread function for the stationary camera is a perfectly uniform $d \times d$ square region. Then Figure 3 shows the psf in the scan and motion directions together with the edge profiles obtained by convolution with an ideal step edge. As before, let $\Delta I = I_{max} - I_{min}$ be the numerator of the expression for contrast. In the horizontal scan direction, the sloped region of the edge profile is given by

$$I(x) = I_{min} + \Delta I(1/2 - x/d), \qquad -d/2 \le x \le d/2,$$

and in the vertical motion direction, the sloped region is given by

$$I(x) = \begin{cases} I_{min} + \Delta I(\frac{1}{2} - \frac{x}{d} - \frac{x^2}{2d^2}), & -d \le x \le 0; \\ I_{min} + \Delta I(\frac{1}{2} - \frac{x}{d} + \frac{x^2}{2d^2}), & 0 \le x \le d. \end{cases}$$

Superimposed on the profiles one may visualize a sequence of sampling points spaced regularly at distances d apart. The maximum slope of the edge profile occurs at $I_{min} + \Delta I/2$, and because of the symmetry of the profiles, only the upper regions need be explored. First consider a small perturbation δ about the threshold T_1 for the first profile. Setting $I(x) = I_{min} + T_1 + \delta$ and solving for x one obtains

$$x = \frac{d}{2} - \frac{dT_1}{\Delta I} - \frac{d\delta}{\Delta I}$$

and

$$\frac{\partial x}{\partial \delta} = -\frac{d}{\Delta I}$$

so that the edge shift for small changes in threshold is independent of threshold and inversely propostional to contrast. In the case of the second profile one obtains

$$x = -d + d\sqrt{2 - \frac{2}{\Delta I}(T_2 + \delta)}$$

and

$$\frac{\partial x}{\partial \delta} = -\frac{d}{\Delta I}\frac{1}{\sqrt{2 - \frac{2}{\Delta I}(T_2 + \delta)}}$$

which now depends on T_2. Figure 4 shows that the edge shift for the vertical direction is minimized at the maximum slope point. In the motion direction, edge shift due to small threshold perturbations increases dramatically as the threshold increases. However, under a reasonable imaging environment, the results shown in Figure 4 demonstrate that the vertical object motion alone is not a serious contributor to measurement error.

Any flattening of the edge profile reduces the edge slope and increases the errors that occur due to random variations or drift in the camera threshold. The major source of error, especially for higher resolution sensors, is optical degradation. The same threshold perturbations shown in Figure 4 can easily affect geometric accuracy much more significantly than motion blur. This is a major reason why it is absolutely essential to use top quality optics in the imaging system.

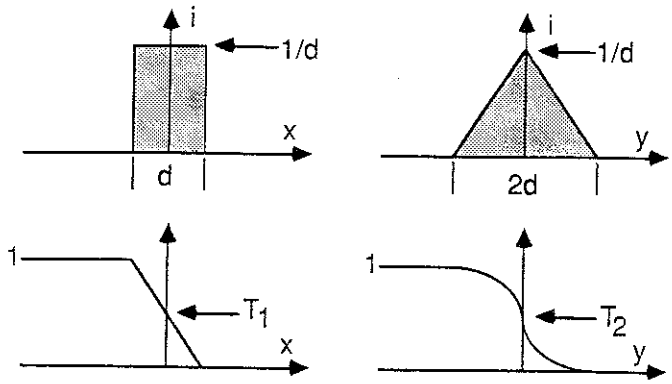

Figure 3 - 1D Camera Response (top) and Corresponding Edge Profiles

2.3 THE 2D FALLACY

Even when binary inspection is applied to scenes that are assumed to be flat, relative to the dimensions involved, this is rarely the case. For example, integrated circuit chips usually have curved edges, which means that the light reflected from the chip edges may appear vastly different from that reflected from the top surface. This may have the effect of a significant flattening of the edge profile, which would make dimensional measurements of chip dimensions vulnerable to threshold variations. Lighting must be carefully designed to avoid the defocussing of edge profiles.

In the case of PC board inspection, even the conductors sometimes need to be treated as 3-dimensional. Light may be scattered from the edge boundaries of the conductors, again spreading out the edge profile. It is also necessary to remember that all non-planar objects are capable of casting shadows, and the smaller the objects, the more imperceptible to the eye these effects will be. Again, unless illumination and imagling are done correctly, threshold instabilities will lead to significant geometric errors.

3 2-DIMENSIONAL GEOMETRY

In this section the major results of the paper are derived. Even though a binary inspection system may have perfect optics and stable thresholds, the resolution of the digital camera system imposes rigid limits to the precision with which the inspection system can function. These limitations are examined here in detail.

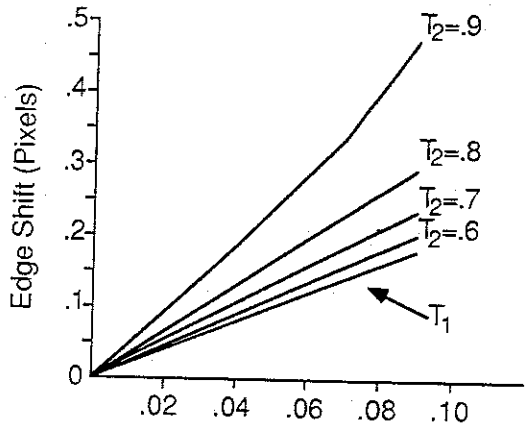

Figure 4 - Threshold Variation

3.1 PERFECTLY REGISTERED WORKPIECES

To introduce the problem, Figure 5 illustrates the pixel level detail of a single scan line across a vertical edge boundary. Suppose that the camera is ideal and that the threshold has been adjusted so that a pixel turns dark when an edge obscures just over 50% of its active area. If pixels 1–5 are light, then the ambiguity δ in the location of the physical edge is exactly d, the distance between pixels in the imaged scan line. If there was no use of don't care regions so that the intensity transition was required to occur exactly between pixels 5 and 6, then the system would guarantee rejection of workpieces that deviated by an amount exceeding $\alpha = d$ from the reference workpiece. However, the system might also falsely *reject* workpieces that differed by an amount ϵ, for any $d \leq \epsilon < 0$, depending on the actual location of the reference edge in the edge ambiguity region. Since in this case rejections would be uncontrolled, the DC regions are required to ensure that good workpieces are accepted.

Figure 5 also shows the tolerance region that would result if pixels 5–6 were defined as don't care pixels, ie., $P = 1$. In the following discussion it is assumed that DC pixels are assigned symmetrically to edges, with P DC pixels on each side. With $P = 1$, this

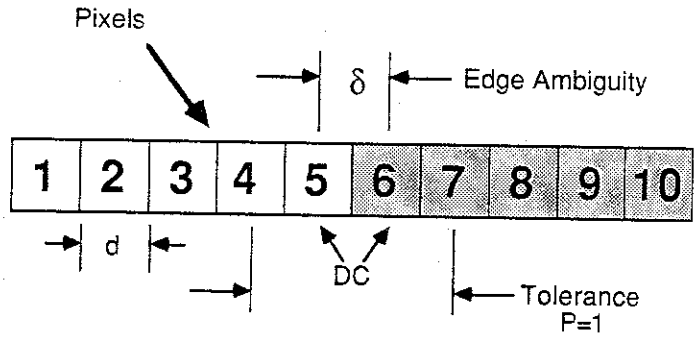

Figure 5 - Basic Tolerance Computation

configuration would guarantee rejection if the test edge location differed from the reference edge location by an amount greater than $\alpha = 2d$, and false rejection could not occur if the deviation was less than $\beta = d$. Thus there is a region of ambiguous behavior of width d, within which the actions of the inspection system are indeterminate. For the 1-dimensional case where there are $2P$ DC pixels at edges, it can be shown that

$$\alpha = (P+1)d$$
$$\beta = Pd$$

where α is the threshold of guaranteed rejection and β is the threshold of guaranteed acceptance. The region of indeterminate behavior has width $\alpha - \beta = \delta = d$, independent of the DC regions.

Looking next at a slightly more complicated case, a similar computation can be performed for the diagonal boundary shown in Figure 6. The edge ambiguity region δ for the reference edge is slightly smaller by a factor of $\sqrt{2}/2$. When $P = 1$, the pixels intersecting the ambiguity region become the don't care pixels, and the tolerance region is extended diagonally by a distance $d\sqrt{2}/2$ in each direction so that the guaranteed acceptance and rejection thresholds are

$$\alpha = (P+1)d\sqrt{2}/2$$
$$\beta = Pd\sqrt{2}/2$$

with a corresponding region of indeterminate behavior of width $\alpha - \beta = \delta = d\sqrt{2}/2$.

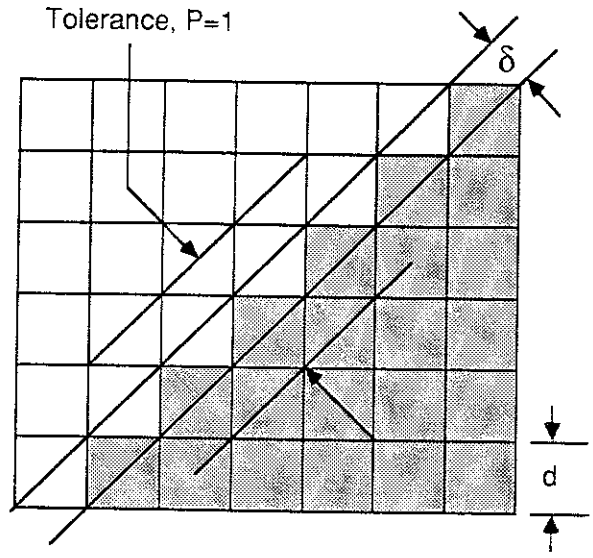

Figure 6 - Diagonal Tolerance Computation

There is a fundamental difference, however, between the computation illustrated in Figure 5 and that in Figure 6 which explains this curious result. The first computation is based on the assumption of a very short edge of length d, while the second computation relys on the fact that the edge is straight and long. In order to deal with edges that lie between vertical and diagonal, it is necessary to distinguish between what are referred to as *long edge models* and *short edge models* because they produce very different results.

Figure 7, which shows edges at a small angle θ from vertical, is helpful in deriving the general results. First, we have the relations

$$L = d\cot\theta$$
$$E = d\csc\theta$$
$$x = d\cos\theta$$

where L is the vertical distance traversed by an edge as it moves one pixel horizontally. Then

$$n = \frac{L}{d} = \cot\theta$$

is the number of pixels traversed by an edge as it moves one pixel horizontally. Then in the **long edge model**

$$\delta = \frac{x}{n} = \frac{d\cos\theta}{\cot\theta} = d\sin\theta \qquad (1a)$$

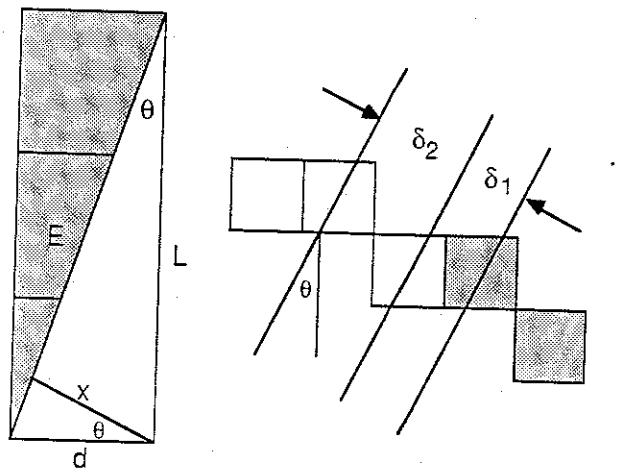

Figure 7 - General Computation

is the normal distance an edge must move before at least one pixel changes intensity. δ is the ambiguity region in both Figures 5 and 6. Then we also have that

$$\alpha = (Px + \delta) = d(P\cos\theta + \sin\theta)$$
$$\beta = Pd\cos\theta \qquad (1b)$$

which yields the correct results for the diagonal edge in Figure 6, provided the edge has length at least $E = d\csc\theta$. However, the region of indeterminate behavior is also δ, which approaches zero as $\theta \to 0$! Thus it will be assumed that the long edge model holds if $E > d\csc\theta$.

In the case of the **short edge model** when $E << d\csc\theta$, one of the regions is considered to be a thin filament normal to the edge boundary. This is illustrated in the right hand drawing in Figure 7. Pixels in this filament are either horizontally adjacent or diagonally adjacent; at $\theta = 0$ they are all horizontally adjacent, and at $\theta = \pi/4$ they are all diagonally adjacent. This gives rise to the corresponding limiting cases $\theta \approx 0$

$$\delta_1 = d\cos\theta$$
$$\alpha_1 = (P+1)d\cos\theta \qquad (2a)$$
$$\beta_1 = Pd\cos\theta$$

and $\theta \approx \pi/4$

$$\delta_2 = d(\cos\theta + \sin\theta)$$
$$\alpha_2 = (P+1)d(\cos\theta + \sin\theta) \qquad (2b)$$
$$\beta_2 = Pd(\cos\theta + \sin\theta)$$

which are consistent with the results obtained from Figure 5.

Equations (1) govern the case where the workpieces to be inspected are known to have long edges that are guaranteed to be straight but which are possibly out of tolerance or in the wrong place. In general, straight edges cannot be guaranteed, and the short edge model described by Equations (2) must be assumed. The worst case occurs for diagonal edges, for which $\delta = d\sqrt{2}$.

To complete the result, one must remember that for a general object under inspection, the short edge model and the long edge model may hold for different parts of the object. For specific measurements one can of course look at specific pixel configurations to determine which model applies. However, for overall performance figures, one must take α to be the maximum of the values in Equations 1 and 2 and β to be the minimum of the values in Equations 1 and 2. Thus the overall result for perfectly registered workpieces are

$$\alpha = (P+1)d\sqrt{2}$$
$$\beta = Pd\sqrt{2}/2 \qquad (3)$$
$$\delta = \alpha - \beta = (P/2+1)d\sqrt{2}$$

In Equations 3, the minimum value of β is attributable to the long edge model, and the maximum value of α is attributable to the short edge model, both in the case of diagonal edges. While one cannot improve worst case performance, average performance can be improved by increasing the value of P chosen for nearly diagonal edges that meet the length requirement for the long edge model. Table 1 gives the worst case results from Equations 3 for $P = 1,\ldots,5$. To set up the inspection system the procedure would be to determine acceptable values of α and β and then to pick a value of P from Table 1. Then the DC mask would be edited to place P DC pixels on either side of each region boundary. Notice that the DC pixels can be placed on the DC mask by the very simple procedure of locating intensity transitions in the horizontal and vertical directions alone and marking P pixels on either side of those transitions.

P	α	β	δ
1	2.83	.71	2.12
2	4.24	1.41	2.83
3	5.66	2.12	3.54
4	7.07	2.83	4.24
5	8.49	3.54	4.95

Table 1 - Worst Case Performance (Pixels)

3.2 IMPERFECTLY REGISTERED WORKPIECES

When dealing with extremely high precision it is generally physically impossible to place workpieces into positions of known registration with the reference workpiece. Therefore reference features are extracted both from the workpiece and from the testpiece to determine the degree of offset between them. Unfortunately this introduces another source of error.

Consider the 1-dimensional case illustrated in Figure 8. At the time the reference image is scanned, the edge position is in the range $b \pm d/2$ and the reference mark is located in the range $r_0 \pm \gamma$ so that the distance between b and r_0 is in the range $m_0 = r_0 - b \pm (d/2 + \gamma)$. All measurements in the reference workpiece and in the test piece are made with respect to the reference mark. Before matching takes place, the two images are shifted so that the corresponding reference marks are aligned as closely as possible. Let us suppose that when the workpiece is matched, the edge appears to be in the same location as before, that is, the light and dark pixels in the reference image match exactly with those in the workpiece. However, the reference mark is located in the range $r_1 \pm \gamma$. Then the corresponding workpiece dimension is in the range $m_1 = r_1 - b \pm (d/2 + \gamma)$ and the maximum measurement difference is $|m_1 - m_0| = |r_1 - r_0| + (d + 2\gamma)$. However, the matching procedure involves shifting the relative positions of the two images by an integral number of pixels to minimize the difference $|r_1 - r_0|$. Then the maximum possible error magnitude when r_0 and r_1 are both real is $d/2+(d+2\gamma)$. Since d is associated with the matching error discussed in Section 3.1, the error attributable to the reference shift is $\epsilon = d/2 + 2\gamma$.

Considering these results, there are two possible ways for using the reference marks. If r_0 and r_1 are real numbers and the subpixelation procedures used are extremely accurate so that $\gamma \approx 0$, then the maximum error approaches $\epsilon = d/2$. On the other hand, if no subpixelation is used so that r_0 and r_1 are always integral, then $\gamma = d/2$, and the maximum error is $\epsilon = d$. In two dimensions, since the horizontal and vertical shifts may each be off by ϵ, then the possible error for an edge at an angle θ from vertical is $\epsilon\sec\theta$, where $0 \le \theta \le \pi/4$.

The actual matching process on the aligned images is the same as before, except that the actual alignment may be off by $\epsilon\sec\theta$. Equations 1 and 2 are modified by adding this amount to all α values and subtracting it from all β values. Noting that the extrema still occur for diagonal edges, Equations 4 give the new error bounds, and these are tabulated in Table 2 for the worst case when there is no subpixelation, that is, when $\epsilon = d$.

$$\alpha = (P+1)d\sqrt{2} + d$$
$$\beta = Pd\sqrt{2}/2 - d \qquad (4)$$
$$\delta = \alpha - \beta = (P/2+1)d\sqrt{2} + 2d$$

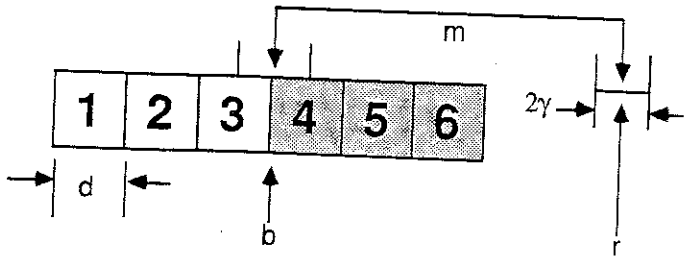

Figure 8 - Positioning Ambiguity

P	α	β	δ
1	4.24	x	x
2	5.66	0.00	5.66
3	7.07	0.71	6.36
4	8.49	1.41	7.48
5	9.90	2.12	7.78

Table 2 - Worst Case Performance (Pixels) with Offsets and no Subpixelation

4 CONCLUSIONS

Many of the problems affecting measurment accuracy of binary inspection systems have been examined from the point ot view of worst case performance, and geometric issues have been treated in depth. The conclusion is that binary inspection systems used for dimensional measurement must be designed with extreme care and can function only in carefully controlled environments. Camera resolution requirements may be considerably higher than one might expect. More work is necessary to characterize and quantify the various types of errors.

REFERENCES

Reinhold, A.G. and VanderBrug, G.J. (1980). Robot vision for industry - the Autovision system. *Robotics Age, 2* (3), 22–28.